Marine Chemistry 113 (2009) 137–147

Contents lists available at ScienceDirect

Marine Chemistry

journal homepage: www.elsevier.com/locate/marchem

Extended time series measurements of submarine groundwater discharge tracers (^{222}Rn and CH_4) at a coastal site in Florida

Isaac R. Santos *, Natasha Dimova, Richard N. Peterson, Benjamin Mwashote, Jeffrey Chanton, William C. Burnett

Department of Oceanography, Florida State University, Tallahassee, FL 32306, USA

ARTICLE INFO

Article history:
Received 4 June 2008
Received in revised form 22 January 2009
Accepted 26 January 2009
Available online 4 February 2009

Keywords:
Subterranean estuary
Permeable sediments
Geochemical tracers
Coastal aquifer
Storm
Time series
Radium isotopes

ABSTRACT

We report the results of an experiment in which we measured ^{222}Rn (15,000 observations), CH_4 (40,000 observations), and associated variables in seawater nearly continuously at a coastal site in the Gulf of Mexico for almost two years. Significant correlations between ^{222}Rn and CH_4 imply that they are derived from a common source, most likely groundwater. However, we were unable to explain the overall tracer variability as a single function of groundwater table height, temperature, tidal range, and wind speed, indicating multiple, overlapping controls on SGD dynamics at this site. Methane and radon concentrations may vary 2-fold in a given well in the subterranean estuary over tidal time scales, demonstrating the complexity of determining SGD endmember concentrations and suggesting that unaccounted for temporal changes in groundwater may explain some of the patterns observed in seawater. Surprisingly, the variability of ^{222}Rn and CH_4 in seawater over short (e.g., hourly) time scales was generally comparable to or even more pronounced than fluctuations over much longer (e.g., monthly) scales. While high tracer concentrations usually occurred during low tide and low tracer concentrations during high tide, this pattern was occasionally inverted or absent indicating that no single model can be used to describe the entire data set. We also describe a sequence of events in which SGD tracers were depleted in coastal waters during storms and regenerated afterwards. We found no increase in radon activities immediately after the largest storm (75 mm rainfall) perhaps because of the short residence times of groundwater in contrast to the ingrowth time of radon. Marine controls appeared to be the most important SGD drivers with only minor influence relating to the shallow and deep aquifers. This implies that seasonal investigations of SGD tracers in the coastal ocean may be masked by short-term variability.

1. Introduction

The coastal ocean is a transitional region where major changes in water biogeochemical conditions occur over relatively small spatial and temporal scales. Long-term, continuous observations of coastal processes have been rarely reported, but such measurements may provide valuable insights into their dynamics. For example, long-term, high-resolution studies of primary production at coastal sites are yielding not only surprising variability, but also fundamental insights into the driving forces that underlie phytoplankton cycles (Smetacek and Cloern, 2008). Long-term measurements (weeks to months) of submarine groundwater discharge (SGD) tracers are particularly scarce, but have proven valuable when attempted (Kim and Hwang, 2002). SGD is defined as any and all flow of water from the seabed to the coastal ocean, regardless of fluid composition or driving force (Burnett et al., 2003). It thus includes both a terrestrial component of fresh groundwater and an oceanic component of recirculated seawater (Burnett et al., 2006; Moore et al., 2008; Mulligan and Charette, 2006).

Even though fresh groundwater discharge directly to the ocean has been estimated to be only a few percent of the global freshwater flux (Burnett et al., 2003; Zektser and Loaiciga, 1993), the input of nutrients is almost certainly more important than that as nutrient concentrations in groundwater are often much higher than those in surface waters.

Recirculated seawater may also be a source of dissolved species (Kroeger et al., 2007; Santos et al., 2008a; Slomp and Van Cappellen, 2004). In a recent analysis, for example, we estimated that the contribution of nitrogen and dissolved organic carbon from the mostly-saline nearshore SGD alone is comparable to the input of new nutrients from local rivers in Florida (Santos et al., 2008a). Significant groundwater inputs of nitrogen, for example, may be a key factor initiating and maintaining phytoplankton blooms in the coastal ocean (Hu et al., 2006; Lapointe et al., 2005). Therefore, groundwater should

* Corresponding author.
E-mail address: santos@ocean.fsu.edu (I.R. Santos).

0304-4203/$ – see front matter © 2009 Elsevier B.V. All rights reserved.
doi:10.1016/j.marchem.2009.01.009

not be neglected in dissolved species budgets even at sites where its volume contribution is small (Santos et al., 2008b).

Groundwater seepage into coastal environments is patchy, diffuse, and temporally variable. The advantage of using natural geochemical tracers to evaluate SGD is that the water column integrates the tracers coming into the system via groundwater pathways. Smaller-scale variations, which are not of regional interest, are thus smoothed out (Burnett et al., 2006; Swarzenski, 2007). We use radon (^{222}Rn) and methane (CH_4) as tracers of SGD. The first significant attempts to use these tracers to assess SGD were conducted in the 1990s (Bugna et al., 1996; Cable et al., 1996a,b). ^{222}Rn and CH_4 may be effective tracers because they are often highly enriched in groundwater relative to surface waters. While ^{222}Rn is radioactive ($t_{1/2}$=3.84 days) and biogeochemically conservative, CH_4 is a product of anaerobic microbial respiration. Methane may work as a SGD tracer at coastal sites in the Gulf of Mexico (Bugna et al., 1996) and some other locations, but it may not be as effective where other sources are dominant (e.g., gas bubbles, production within the water column, etc.). For example, methane was discarded as a tracer in West Neck Bay (New York) and Mangueira Lagoon (Brazil) because it was low in local oxic groundwater (Dulaiova et al., 2006; Santos et al., 2008c). Even though radon and methane may have different geochemical pathways, positive anomalies of both gases are likely due to SGD.

We report here the results of an experiment in which we measured ^{222}Rn, CH_4, and associated variables continuously at a coastal site in Florida for almost two years. Based on these observations, we attempt to understand the effect of short- and long-term processes driving the input of SGD tracers into the coastal zone. While most of our current understanding about short-term (tidal scale) SGD dynamics is derived from ^{222}Rn (Burnett et al., 2008; Burnett et al., 2007; Dulaiova et al., 2006; Kim and Hwang, 2002) and seepage meter (Sholkovitz et al., 2003; Taniguchi, 2002; Taniguchi et al., 2008) measurements, most seasonal SGD tracer investigations have been based on radium isotopes (Beck et al., 2007; Charette, 2007; Hougham et al., 2008; Kelly and Moran, 2002; Loveless et al., 2008; Moore, 1997; Moore, 2007; Moore et al., 2006). Because radium sampling is labor-intensive and requires the filtration of large volumes of water (about 100 L), those previous seasonal studies were often based on one sampling each season and relied on the assumption of steady-state SGD inputs over the short-term (e.g., hours to days). As is now widely recognized, resolving seasonal or longer-term trends from traditional quarterly or even monthly surveys can be extremely difficult.

The advent of automated measurement systems now allows high-resolution ^{222}Rn and CH_4 analysis at one location over time (Burnett et al., 2001; Garcia and Masson, 2004). Kim and Hwang (2002) took advantage of these capabilities and monitored ^{222}Rn and CH_4 off a rocky–sandy shore in Korea for nearly one month in the summer and in the fall, probably the longest and the most detailed SGD tracer data set currently available. These authors suggested that SGD increases from neap to spring tide during the wet, but not during the dry seasons. Our longer-term data set allows us to assess whether such relationships may be recognized at a coastal plain site in northern Florida dominated by diffuse groundwater seepage. As suggested from seasonal radium sampling at other locations (Kelly and Moran, 2002), one may expect that tracer concentrations correlate with the groundwater table on land if terrestrial forces control SGD.

2. Methods

2.1. Study area

The experimental site is located in the northeastern coastal Gulf of Mexico (Turkey Point). We carried out our measurements at the Florida State University Coastal and Marine Laboratory (FSUCML), located approximately 80 km south of Tallahassee, Florida. This is a well-known area for the presence of both diffuse seepage near shore (from the unconfined aquifer) and submarine springs further offshore (from a karstic confined aquifer). The area sits atop a layered dolomite and limestone platform that hosts the Floridan Aquifer, considered one of the most prolific aquifers in the world. This aquifer is overlain by a clay, silt, and sand surficial, unconfined aquifer, which is recharged locally by precipitation. Annual mean precipitation for the region is ~150 cm, although the annual totals were considerably less during the study period (2006: 87 cm; 2007: 62 cm), leading to a large drought in the area. Rainfall peaks are usually from June to October, while the lowest precipitation rates occur in November/December and March to May. The tides here are mixed and semi-diurnal with an average range of 0.85 m. The seafloor is characterized by gently sloping topography away from the coast resulting in a water depth of ~2 m as far as 1000 m offshore (Cable et al., 1997; Lambert and Burnett, 2003).

2.2. Data collection

Fig. 1 shows a schematic representation of our observation strategy. We measured seawater salinity, temperature, CH_4 and ^{222}Rn from 18 Nov 05 to 15 Oct 07. Seawater was continuously pumped to the laboratory from ~1.6-m water depth at a spot 300 m offshore. Weekly maintenance and data retrieval guaranteed a quasi-continuous data set (except for methane). The main problems encountered during the deployment were associated with growing barnacles and other organisms along the pipeline. By periodically cleaning key parts of the pipeline (e.g., intake, pump, and outlet), we prevented clogging and maintained a reasonable seawater flow rate (>5 L/min). Any suspicious data, usually associated with little or no water flow when there were problems with the pump, were discarded. The system was checked every morning and late afternoon. An efficient way to ensure that water was flowing into the lab was to compare the temperature of seawater and air inside the lab, as stagnant water acquires the air-conditioned lab temperature within a few minutes.

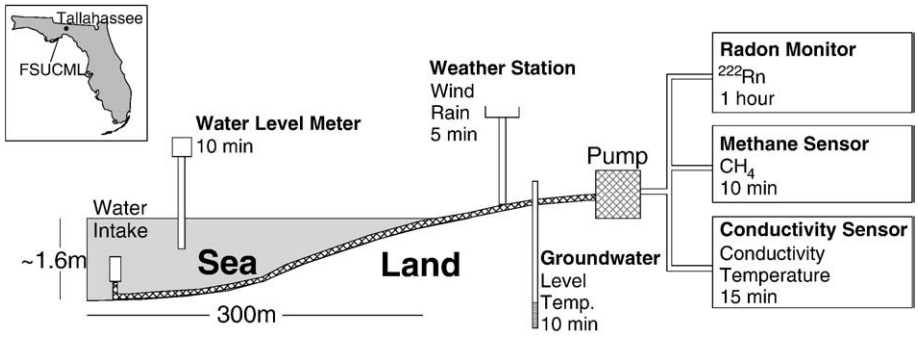

Fig. 1. Schematic representation of our monitoring system in FSUCML.

Water depth at the intake was measured with an ultrasonic water level meter. Precipitation and wind speed data were obtained online (www.wunderground.com) from a weather station located at Alligator Point, about 10 km from our seawater monitoring system. Groundwater level, temperature, and conductivity were monitored using CTD Divers (Van Essen instruments®). We report results from two local piezometers. One of these (well A2), is a 3 m deep, freshwater well located ~20 m onshore from the high tide mark. The other (well BC1) is a 3.7 m deep, brackish water well located 40 m seaward from the high tide mark.

We measured ^{222}Rn with a portable continuous Rn-in-air monitor (RAD7, Durridge Company) adapted for Rn-in-water measurements. Radon activities were determined by counting its alpha-emitting, positively charged radioactive daughter (^{218}Po), which is detected by a silicon detector in a discrete energy window. The approach of such a monitor is basically the equilibration of a stream of flowing water with a stream of air that is re-circulated through the RAD7. Since the method relies on the equilibration between the Rn-in-air and the Rn-in-water, one must know the Rn partitioning between the gas and the liquid phase. Such equilibrium is temperature-dependent and can be easily determined (Burnett et al., 2001).

For the measurement of dissolved methane, we used a METS sensor (Capsum Technologies, Germany). The sensor relies on the adsorption of CH_4 molecules on a tin dioxide semiconductor detector, which results in a resistance variation (Garcia and Masson, 2004; Grunwald et al., 2007). Hydrocarbon molecules diffuse through a silicone membrane into the detector chamber. The detection limit, as provided by the manufacturer, is 0.02 μM. The sensor was installed in the lab inside a 1 L cylinder, which was constantly supplied with seawater and overflowed at a rate of about 3 L/min. The moderate turbulence ensured a constant flow of seawater to the sensor, preventing the membrane from fouling. The membrane was replaced approximately every month or when bio-fouling could not be removed by a weak water jet. Close inspection of the data before and after membrane replacements indicated some drift in concentrations within the first several hours of a new membrane; such data was

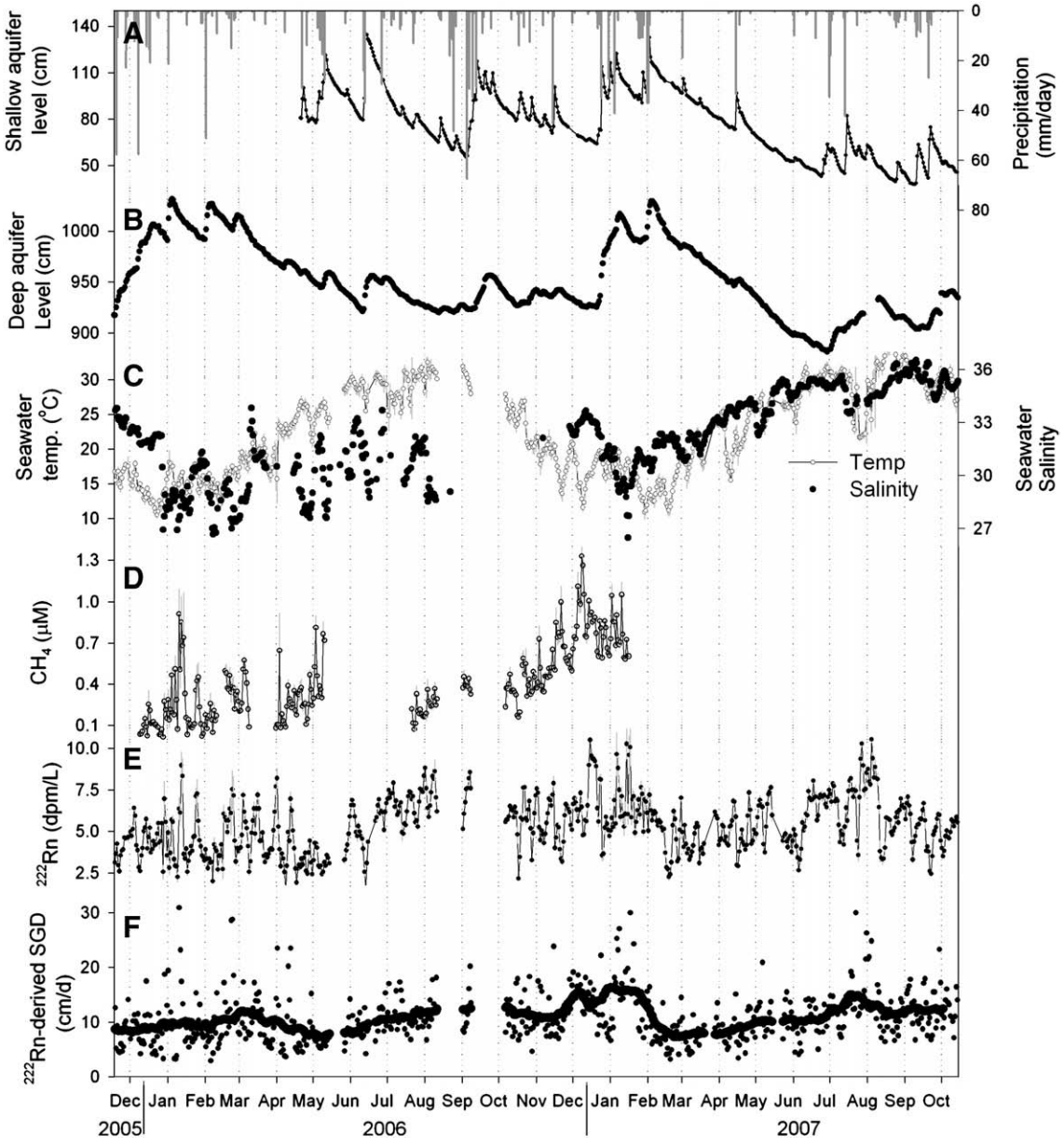

Fig. 2. Daily averages of selected variables between November 2005 and October 2007. (A) shallow groundwater level (well A2) and precipitation; (B) deep aquifer level (USGS well in Crawfordville, Fl); (C) seawater temperature and salinity; (D) CH_4; (E) ^{222}Rn; and (F) ^{222}Rn-derived SGD rates.

Table 1
Descriptive statistics of variables measured from 18 Nov 2005 to 15 Oct 2007

	Radon	Methane	Depth	Wind speed	Temperature	Salinity	Atmospheric evasion	Mixing losses	Advection
	dpm/L	μM	m	m/s	°C		dpm/m^2/h	dpm/m^2/h	cm/d
Mean	5.4	0.46	1.8	3.8	22	32.3	218	208	11.0
Median	5.3	0.40	1.8	3.2	22	32.4	136	142	8.8
Standard deviation	1.8	0.32	0.3	2.6	7	2.5	244	268	10.2
Percentile 25%	4.1	0.19	1.6	2.1	16	30.6	65	35	3.6
Percentile 75%	6.5	0.67	2.0	5.1	29	34.4	276	285	15.5
Maximum	14.6	2.49	2.7	19.5	37	37.2	2474	8202	154.7
Minimum	1.2	0.01	0.5	0.0	9	22.6	0	0	0.0
Valid observations	14,955	39,948	90,631	179,305	59,919	48,361	14,928	14,928	14,928

omitted. In most cases, however, the record returned to a predictable pattern after maintenance. We used two METS sensors throughout this project which were both calibrated against gas chromatography. For calibration, methane standards were bubbled through tap water that was monitored with the METS sensor. Grab samples for CH_4 analysis were collected in Wheaton glass bottles and concentrations were determined using a Shimadzu 8A flame ionization detection (FID) gas chromatograph with a 1 mL sampling loop and HayeSep Q (80-100 mesh) column (Bugna et al., 1996). After about 6 months of deployment, the first METS was sent to the manufacturer for repair, as its casing was deteriorating. The second sensor (deployed between July 2006 and January 2007) also started deteriorating after about 6 months of deployment, at which point we decided to stop methane monitoring.

The available time series consist of variables measured at different time intervals (Fig. 1). Since the time step is not constant, hourly averages were derived to allow for the assessment of relationships among these variables.

3. Results and discussion

3.1. Tracer correlations in seawater

Fig. 2 shows the time series obtained and Table 1 provides descriptive statistics of these data. The ocean depth at the seawater intake ranged between 0.5 and 2.7 m. The salinity median was slightly higher than its average, probably influenced by a few strong rain events. The A2 well level varied between 35 and 160 cm above the North Atlantic Vertical Datum (NAVD 1988). Seawater temperature exhibited the expected seasonal pattern. The local water table, represented by well A2, responded very quickly to rainfall events and was not affected by tidal fluctuations. Groundwater salinity in this well (not shown) oscillated around 0.4 and had no clear seasonal trend. We also examine groundwater level from a USGS well located in Crawfordville, about 25 km away from FSUCML. This well has a typical sinusoidal seasonal pattern and represents our best proxy of the influence of the deep Floridan aquifer on SGD tracer concentrations.

Histograms indicated that while the ^{222}Rn distribution in seawater was normal, methane concentrations were skewed to the left (Fig. 3). Even though ^{222}Rn and CH_4 have different geochemical behavior and statistical distribution, the significant correlation (n=6,580; r=0.39; p<0.01) between them (Fig. 4) implies that they are often derived from a common source. Hence, groundwater input is probably the most important factor controlling their temporal distribution, confirming earlier observations (Bugna et al., 1996). Fig. 4 also indicates that when methane concentrations approach zero, some radon (~1000 dpm/m^3) can still be detected. This likely indicates that other significant sources exist for radon (^{226}Ra decay and diffusion across the sediment–water interface), but not for methane. An alternative explanation would be that methane is removed from the aquatic system faster than radon. At this study area, the probable sinks of methane are in-situ oxidation and flux across the air–sea interface. Methane oxidation was reported to be one order of magnitude lower than the flux to the atmosphere at the same site in the Gulf of Mexico (Bugna et al., 1996). Therefore, atmospheric evasion is probably an important methane sink at this site, as indicated by the negative methane–wind speed trends (Fig. 5). We thus suspect that some variations from the trend are largely controlled by wind speed, which may affect methane more than radon. In equilibrium conditions (20 °C), the water:air concentration ratios for radon and methane are about 0.2 and 0.03 (Burnett et al., 2001; Yamamoto et al., 1976), respectively, so methane can degas much faster than radon. This is supported by methane's steeper slopes when it changes from a high to low concentration (see Section 3.4). The observation that methane approaches zero while radon does not may simply be due to groundwaters becoming oxic, stopping the production of methane, but not of radon.

Though both tracers usually follow the same distribution pattern, the relative standard deviation is much larger for methane (Table 1). This may be explained at least partially by the fact that the CH_4 sensor responds quicker to concentration changes than the RAD7 and by its

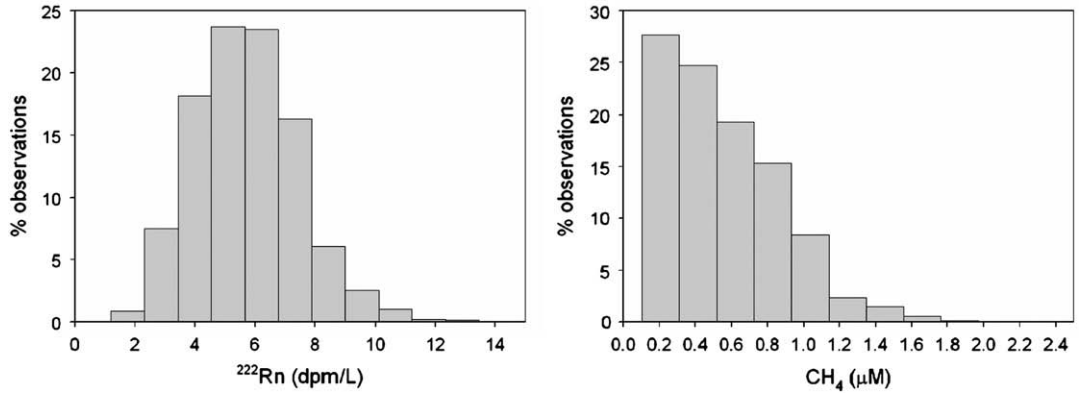

Fig. 3. Histograms showing the frequency distribution of ^{222}Rn and CH_4.

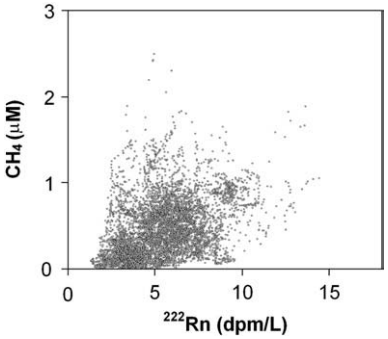

Fig. 4. Scatter plot between CH_4 and ^{222}Rn.

shorter measurement integrations (10 min relative to 1 h for ^{222}Rn). According to the manufacturer (Franatech®), the response time of the METS sensor is less than 5 min, while our radon monitor responds to a concentration change within 20–30 min (Burnett et al., 2001). Even though we have not performed detailed experiments to test the response time of the METS sensor, the time series plots (see Section 3.4) clearly indicate a response time of the METS sensor shorter than the RAD7. Experiments involving towing a METS sensor and a radon monitor further indicate a faster METS response both from low to high and from high to low concentrations (Dimova, N. unpublished data). While the METS sensor response is driven by diffusion of hydrocarbon molecules across a membrane (faster diffusion for turbulent waters), the RAD7 response is controlled by air:water equilibrium and radioactive decay of radon daughters, explaining the difference in response times.

3.2. Groundwater tracer concentrations

Part of the deviations from linearity in the radon–methane scatter plot (Fig. 4) may be explained by short- and long-term changes in the groundwater endmember concentrations. While radon in sediments depends essentially on the physical properties and ^{226}Ra content of sediments, methane production is controlled by microbial activity in anoxic conditions which is likely to be strongly influenced by temporal fluctuations. In May 2006, we conducted an experiment to test whether groundwater endmember concentrations in the subterranean estuary can be variable over short time scales. We performed radon and methane time series measurements in groundwater sampled from four wells located in the intertidal zone at depths ranging from 2 to 3.5 m. We also collected samples from a seepage meter located 50 m offshore from the high tide mark.

The results indicated that radon may vary 2-fold in a given well within several hours, as illustrated by a 2.2-m deep well located at the high tide mark (Fig. 6). Radon in seepage meter water does not fall on a simple mixing line with the monitoring wells sampled on shore (Fig. 7). While our results demonstrate a remarkable short-term variability, recent investigations highlight that the groundwater radon endmember can also be highly variable over longer time scales. Monthly sampling of a subterranean estuary in Massachusetts, for example, indicated radon activities ranging between 50 and 1600 dpm/L. Groundwater radon in that case was suggested to be linked with the accumulation of ^{226}Ra, which, in turn, is regulated by manganese oxide accumulation (Dulaiova et al., 2008).

Methane in groundwater was also highly variable over short time scales (Fig. 6). Even though methane correlated with salinity within an individual well (Well AB2; $n=10$, $r=0.68$; $p<0.05$), no clear trends emerge if we plot all the data together (Fig. 7). This suggests that in situ methane production rates are faster than mixing between different water masses in the coastal aquifer. The seepage meter water had concentrations one order of magnitude higher than the intertidal zone wells, probably as a result of methane production driven by labile organic matter remineralization in near-surface coastal sediments. Whether this is an artifact of the chamber causing a reducing environment is unclear (Cable et al., 2006). A previous investigation at the same general area (Bugna et al., 1996) found average methane concentrations of 61 μM in wells, sinkholes and springs, a value larger than our intertidal zone wells (average 6 μM), but comparable to the seepage meter water (average 93 μM).

The mechanisms driving SGD tracer variability in the subterranean estuary over short-time scales are still unclear, but are probably related to mixing of water masses with different salinities. Time series sub-bottom resistivity surveys in the intertidal zone of FSUCML and other sites suggest decimeter-scale tidal modulation of the aquifer (Swarzenski et al., 2007). The large spatial and temporal variability we observed in the subterranean estuary radon and methane concentrations demonstrates the complexity

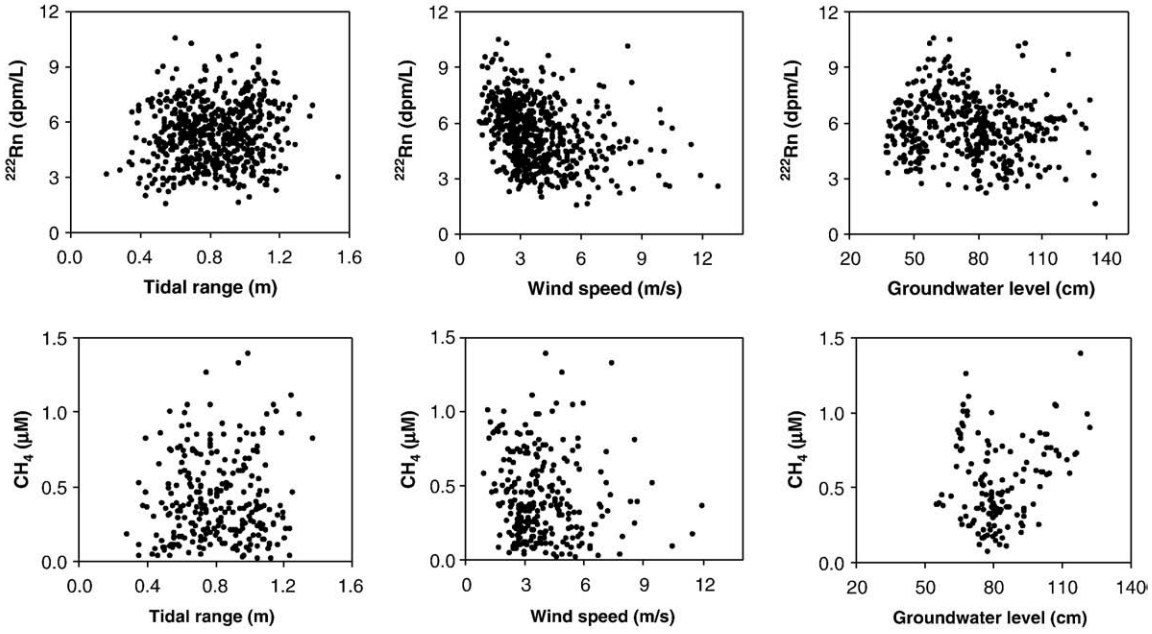

Fig. 5. Scatter plots showing the relationships between CH_4 and ^{222}Rn and possible controls (tidal range, wind speed, and shallow groundwater level). Each point represents an integration of 24 h periods.

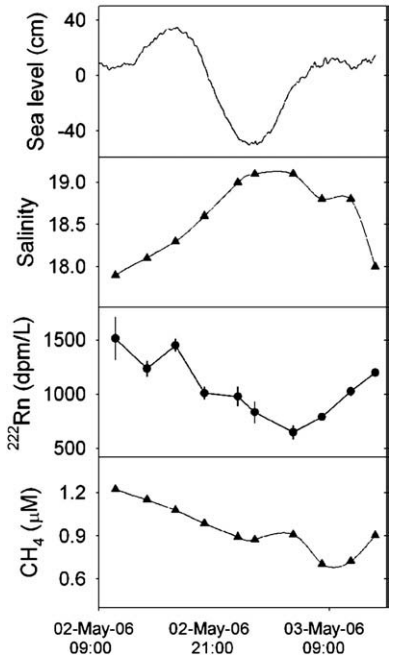

Fig. 6. Results of salinity, radon, and methane time series in groundwater from well AB2, a 2.2-m deep well located at the high tide mark.

of determining SGD endmember concentrations, as previously illustrated for radium isotopes (Gonneea et al., 2008). In many situations, the groundwater concentration represents the largest uncertainty for estimating tracer-derived SGD (Burnett et al., 2006; Burnett et al., 2007). We thus recommend that endmember concentrations be determined concurrently with surface water measurements in future investigations.

3.3. Modeling SGD rates

We used the radon time series observations to model SGD rates following an approach described in detail elsewhere (Burnett and Dulaiova, 2003). This approach has been previously applied to shorter data sets obtained at the FSUCML and some other sites (see review by Burnett et al., 2006). Briefly, the change in radon inventory over time, after making appropriate allowances for losses (decay, mixing with offshore waters and atmospheric evasion) and inputs (SGD and ^{226}Ra decay in the water column) was used to estimate fluxes. Calculated ^{222}Rn fluxes (in units of dpm/m^2/day) were converted to water advection rates (in units of cm^3/cm^2/day, or cm/day) by dividing the total ^{222}Rn fluxes by the estimated groundwater radon endmember concentration. We assumed a constant groundwater endmember, as estimated from sediment equilibration experiments (129 dpm/L; Lambert and Burnett, 2003).

Descriptive statistics for the mixing and atmospheric radon losses, as well as the estimated SGD rates are presented in Table 1. On average, mixing losses contribute 49% of radon losses, with the remaining due to atmospheric evasion. In this model, radon decay becomes negligible as the measurement time steps are very short (1 h) compared to the radon half-life (3.8 days). Other sites where this model has been applied had a relatively higher contribution of mixing losses. For example, at Carmel Coast, Israel, radon mixing losses were about 3 times greater than those from evasion (Weinstein et al., 2007), while at a fractured aquifer site (Ubatuba, Brazil), mixing losses were one order of magnitude greater (Burnett et al., 2008). The relatively low contribution of mixing to the total radon losses at the FSUCML site can be attributed to this environment being relatively sheltered, as offshore bars prevent significant mixing and wave action nearshore.

The temporal variability of radon-derived SGD rates is presented in Fig. 2F. Similar to the raw radon activities, a very high degree of variability is associated with the estimated SGD rates. The ranges in SGD rates over daily (and often over hourly) time scales repeatedly encompassed the whole range observed over the 23 months of observations. Modeled SGD rates were significantly correlated with ^{222}Rn concentrations (r=0.62, p<0.01, n=696 days, Fig. 8). Even though such a correlation seems intuitive, one might expect a larger scatter as our model is based on the change in the ^{222}Rn inventory over time (flux, not concentration) rather than on the magnitudes of the ^{222}Rn concentrations themselves.

The major limitation of our radon-derived SGD rates is related to the fact that we have to assume a constant groundwater endmember. To determine such an endmember, one can rely on measurements from monitoring wells, fluids sampled from piezometers or seepage meters offshore, or perform sediment equilibration experiments as described elsewhere (Corbett et al., 1998). In areas where seepage through sandy sediments is the main mode of discharge, such as at the FSUCML site, equilibrating seawater with sediments should be an excellent way to estimate the radon activity of advecting fluids. With flow rates on the order of a few centimeters per day, there should be ample time for the fluids to equilibrate with ^{226}Ra in the solid phases of the sediment (Burnett et al., 2007). The sediment equilibration experiments results for this site (129±50 dpm/L; n=6) are slightly higher than seepage meter radon concentrations (ranging from 80 to 115 dpm/L; Fig. 7), supporting our choice of the radon endmember. However, if one used either well B1 or B5, the endmember activity could have been overestimated by one order of magnitude.

3.4. Short-term fluctuations: the influence of tides

Surprisingly, the variability of ^{222}Rn and CH_4 over short time scales was comparable to or even more pronounced than fluctuations over longer time scales. Frequently, both tracers are closely related to each other and to the water level (Figs. 9 and 10). High tracer concentrations usually occur during low tide and low tracer concentration during high tide. This is likely due to a combination of two processes: (1) a change in the hydraulic gradient in response to the tidal fluctuation

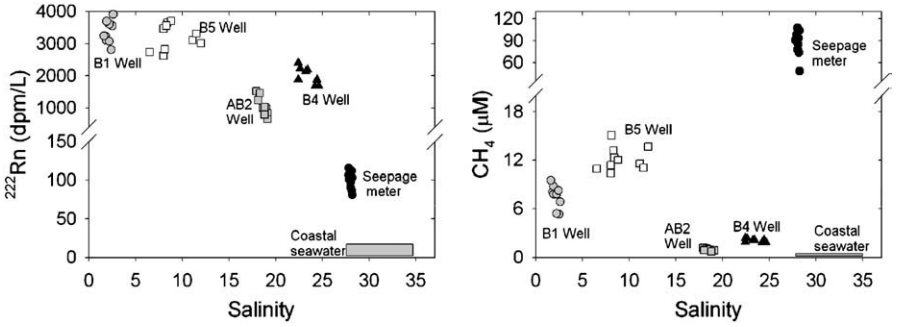

Fig. 7. ^{222}Rn and methane versus salinity in groundwaters of four wells, seepage meter, and seawater. Note that the break in scale distorts the relationships somewhat.

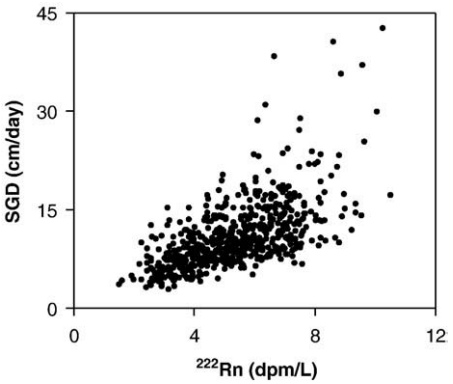

Fig. 8. Scatter plot between SGD rates and ^{222}Rn concentrations averaged over 24 h periods.

(e.g., higher gradients during low tide); and (2) recirculation of seawater through the shallow aquifer in response to tidal pumping (Charette et al., 2008). Even though ^{222}Rn and CH_4 usually follow the same pattern, there are many periods in which discrepancies were observed. Fig. 11, for example, shows a situation when methane peaked at the low tide, but radon did not follow the same pattern, illustrating the complexity of this data set.

Occasionally, higher tracer concentrations coincided with high tides (Fig. 10). This unexpected pattern has not been described before and we can only speculate about its causes. We suspect that it is related to sporadic SGD inputs from nearby offshore springs. Even though SGD at this site appears to be dominated by near shore diffusive inputs (Burnett and Dulaiova, 2003; Lambert and Burnett, 2003), springs may be a groundwater source to shelf waters (Moore, 2003; Swarzenski et al., 2001). We suspect that these offshore springs have not been discharging continuously during the recent drought, but when they did discharge, the waters may have advected onshore during high tides. This could explain the high concentrations at high tide shown in Fig. 10.

In addition to water level fluctuations, wind speeds will also control gaseous SGD tracer fluctuations over short-time scales. Losses to the atmosphere may dramatically decrease the seawater concentrations of ^{222}Rn and CH_4, as occurred on 25 Dec 2006 (Fig. 9) and

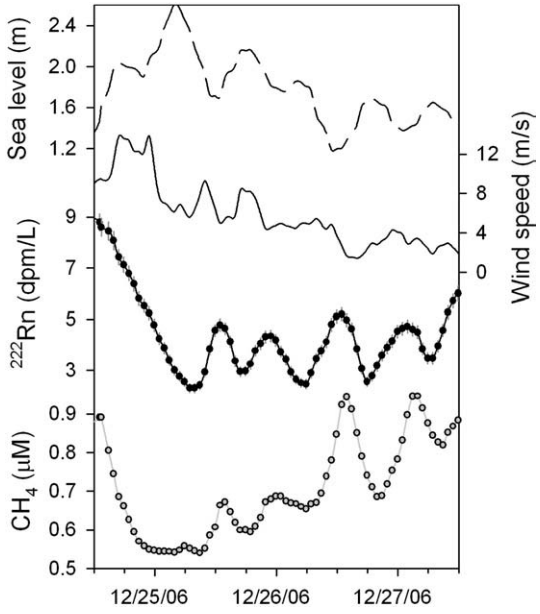

Fig. 9. Time series of groundwater tracers highlighting a situation when radon and methane concentrations decrease abruptly, probably as a result of high wind speeds, and later follow the tidal patterns.

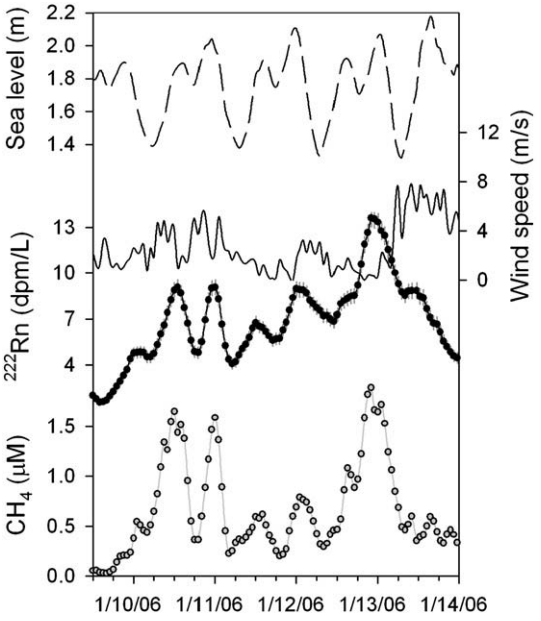

Fig. 10. Time series of groundwater tracers highlighting a situation in which radon and methane reach high concentrations and follow the same pattern.

during the passage of storms (see Section 3.5). In spite of the scattered nature of the data (n=616, r=0.32 for radon; n=254; r=0.11 for methane), averages of SGD tracers plotted against wind speeds show a negative trend (Fig. 5). The wind speeds at this study area exhibited no clear seasonal pattern, so these negative trends reflect short-term processes driven by local weather events rather than a seasonal climate cycle.

Evidence for tidally-driven SGD tracer variability in the coastal ocean has emerged in the last few years (Burnett et al., 2008; Dulaiova et al., 2006; Kim and Hwang, 2002). For example, in Florida Bay (Chanton et al., 2003) and in Kahana Bay, Hawai i (Garrison et al., 2003), maximum ^{222}Rn concentrations were associated with low tides, when maximum SGD rates occur. Short-term SGD oscillations have also been observed from seepage meters in a few other settings (Sholkovitz et al., 2003; Taniguchi, 2002, 2008). Our results indicate

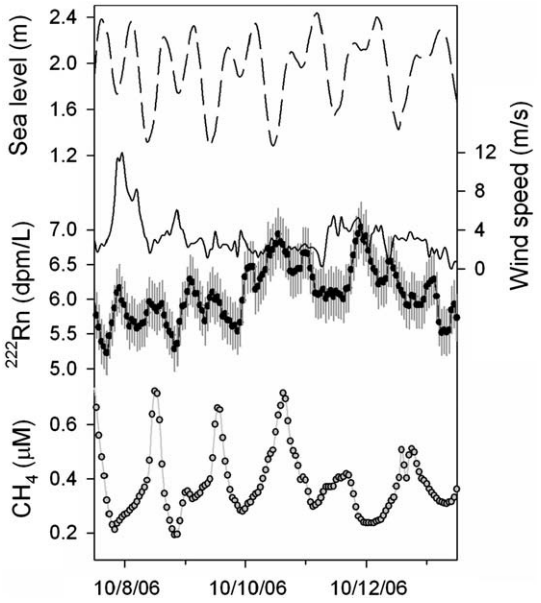

Fig. 11. Time series of groundwater tracers in a situation when methane peaks at the low tides, but radon does not follow the same pattern.

that more complex and variable relationships between SGD and tidal oscillations may appear if observations are made for a sufficient length of time. No single pattern (e.g., high tracer concentrations at low tide) can be used to describe our whole data set.

At a site in South Korea, ^{222}Rn and CH_4 concentrations were higher during spring tide in the summer, but not in the fall, suggesting that the tidal pumping plays a major role in the bi-weekly fluctuations of SGD (Kim and Hwang, 2002). This was also observed during a seepage meter study in Osaka Bay, Japan, where not only a semi-diurnal to diurnal tidal relationship to SGD exists, but also a bi-weekly variation in flow reflecting the neap–spring lunar tidal cycle (Taniguchi, 2002; Taniguchi and Iwakawa, 2004). By focusing on selected parts of the data set, similar patterns can be described for FSUCML. For example, in Mar–Apr 06 and Aug–Sep 07 ^{222}Rn concentrations were not in steady state but oscillated with an apparent period of ~15 days (Fig. 2), likely reflecting lunar tidal cycles.

We suspect that two processes may explain higher tracer concentrations during spring tide: enhanced tidal pumping forces and/or longer tidal period, which would provide more time for ^{222}Rn and CH_4 regeneration in sediments. Neap tides at FSUCML are characterized by two symmetrical cycles per day, with ~6 h intervals between the high and low tides, and smaller tidal ranges (~50 cm). Spring tides at this site, however, are characterized by a greater tidal range (~90 cm) and only one significant cycle per day. As a result of the inconstant tidal periodicities, correlations between tidal ranges and SGD tracer concentrations for our whole data set are hampered. The lack of significant correlations (n=616, r=0.10 for radon; n=254; r=0.06 for methane; p>0.01) between groundwater tracers and tidal ranges (Fig. 5) may be considered evidence that enhanced tidal pumping during spring tide is not important here. However, we suspect that there are additional factors beyond tidal range needed to explain tracer concentrations. Modeling of a hypothetical aquifer (Li and Jiao, 2003) indicated that seawater that infiltrates the unconfined aquifer during high tide is divided into two parts. Part returns immediately to the sea, driven by the water table gradient, while the rest leaks into a more confined aquifer through a semi-permeable layer and returns to the sea through the confined aquifer driven by the mean head gradient. It would follow that the water returning later to the sea is enriched in SGD tracers relative to the fraction that returns immediately. If this is indeed true, during spring tide (longer period), a larger volume of water would leak into the confined aquifer and have a longer time in contact with sediments, favoring tracer enrichment in this saline groundwater. In order to properly quantify the influence of spring–neap cycles on SGD tracer concentrations, one should compare the residence time of the water emanating from sediments with tracer regeneration rates.

3.5. The influence of storms

We successfully obtained hydrological and geochemical data during the passage of several storms. Investigations about the influence of storms on coastal systems often focus on the redistribution of sediments. An important, but usually neglected consequence is the alteration of coastal groundwater processes, such as saltwater intrusion and SGD (Hu et al., 2006; Moore and Wilson, 2005; Smith et al., 2008). We show data from the largest storm that occurred in the area during our monitoring period. Tropical Storm Alberto was formed in an area between the Yucatan Peninsula and Cuba on 10 Jun 06. It moved northward and reached the coast of Florida on 13 Jun 06, just a few kilometers east of our site (Fig. 12). The storm reached its peak intensity with wind speeds of 31 m/s and a minimum pressure of 995 mb about 180 km south of the coast (Avila and Brown, 2006). The highest recorded storm surge occurred at Cedar Key (1.2 m), located nearly 200 km southeast of FSUCML. We observed a sequence of four stages that occurred during the passage of this and other storms (Fig. 13):

(1) *Pre-storm* (before 11 Jun 10:00): No evidence of Alberto's influence. A2 well level, temperature and salinity are nearly stable. Radon in the coastal waters followed its regular temporal distribution pattern, as discussed in Section 3.2.
(2) *Storm surge* (from 11 Jun 10:00 to 12 Jun 17:00): Sea-level and BC1 well level increased due to high offshore winds. Coastal radon concentrations decreased sharply, apparently due to dilution with low Rn offshore water and higher atmospheric emanation rates driven by increasing winds. In spite of having its screen 3.7 m below the sediment–water interface, BC1 well level perfectly mimicked sealevel, showing that high exchange process must occur in this area. In addition, the salinity in BC1 suddenly increased, indicating that seawater intruded into the subsurface.
(3) *Rainfall* (from 12 Jun 17:00 to 14 Jun 00:00): All of the storm-associated rainfall occurred during this period (total of 75 mm). The atmospheric pressure dropped and rose to its initial level within 24 h. A2 well level increased rapidly (77 cm) as a response to the rain event. Comparing the well level change with the total rainfall and assuming a local porosity of >0.1, we can estimate that ~100% of the rainfall infiltrated into the

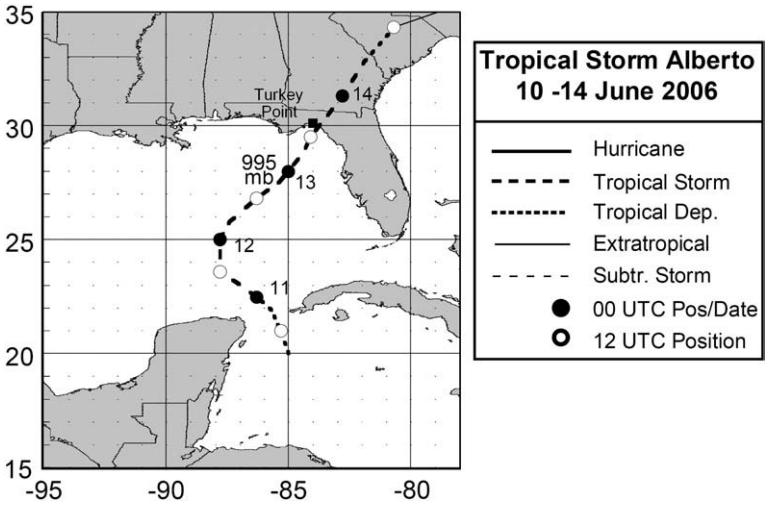

Fig. 12. Tropical Storm Alberto track, 10–14 June, 2006 (redrawn from Avila and Brown, 2006).

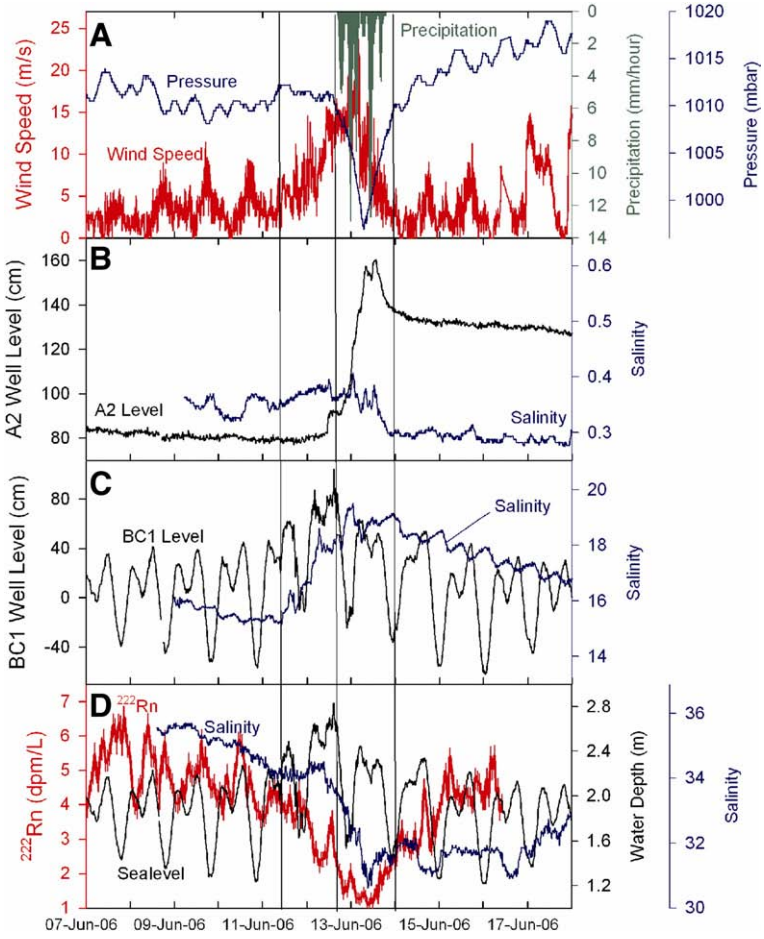

Fig. 13. Time series of atmospheric (A), hydrological (B and C), and ocean (D) conditions during the passage of Tropical Storm Alberto. The vertical lines represent the limit of the 4 stages defined in Section 3.6. (A) wind speed, atmospheric pressure, and precipitation; (B) A2 well level and salinity; (C) BC1 well level and salinity; (E) ^{222}Rn and salinity in coastal water and depth at the seawater intake.

aquifer. Therefore, in spite of the torrential rain, little to no water was available for surface runoff. Radon reached its minimum level and began to recover in the water column in response to decreasing winds. Concurrent with rising barometric pressures, sea level returned to its normal stand and the wind velocities dropped. All these processes favor rapid radon buildup in the water column from SGD inputs. Seawater salinity reached its minimum as a result of rainfall dilution.

(4) *Post-storm* (after 14 Jun 00:00): Most environmental conditions were stable and similar to those during the pre-storm stage. However, the water table was much higher. A2 well level decreased at a rate of nearly 2 cm/day, so in about 35 days it reached its pre-storm level. Daily oscillations of the coastal radon levels followed the same pattern observed before the storm, indicating no immediate influences of higher water tables on SGD tracer concentrations.

Contrary to radon in seawater, subsurface salinity did change after the storm (Fig. 13C). The salinity of well BC1 increased from 16 to 19 due to enhanced seawater intrusion into the coastal aquifer associated with the storm surge. After the storm, BC1 salinity not only followed its daily oscillation pattern, but also started decreasing probably due to the influence of a higher terrestrial water table. Temperature records in groundwater off South Carolina indicated that a considerable volume of water in the aquifer was replaced with warmer ocean water during the passage of a storm (Moore and Wilson, 2005). This is consistent with our BC1 well data, implying that the processes observed in FSUCML may also occur over larger spatial scales. A recent investigation in central Florida suggests that tropical storms influence the biogeochemical setting of the subterranean estuary by changing the residence time of seepage waters due to the landward migration of the mixing zone (Smith et al., 2008). Therefore, in addition to changing salinities, we suspect that the disturbance caused by storms may temporally alter the SGD tracer endmember concentration, further complicating the interpretation of these results. Another major complication to the interpretation of this data set refers to sediment resuspension during storms, as it may represent a possible source of both radon and methane to the overlying water column.

This sequence of events shows that Tropical Storm Alberto controlled the temporal dynamics of meteorological, hydrological, and geochemical parameters measured in groundwater and surface waters at FSUCML. Surprisingly, there was no detectable increase in radon concentrations within a few days (Fig. 13D) or weeks (Fig. 2) after the storm. If fresh SGD was important here, one might expect an increase in seawater radon a few weeks after the storm as this would be enough time for radon to regenerate in the aquifer and the water table was still higher than the average. The higher seawater recirculation during the storm indicated by salinities in well BC 1 and suggested by Moore and Wilson (2005) cannot be deduced from our seawater radon observations because we did not monitor radon endmember concentrations in the aquifer. It is likely that groundwater radon decreased during the storm as a result of lower groundwater residence times. A recent paper (Hu et al., 2006) provided new insights into the possible connections between storms and SGD. They

suggested that hurricanes may trigger higher than average fresh SGD rates along the Florida coast. While this may hold true for areas where groundwater discharge is controlled by the terrestrial water table, it does not seem to be the case at the FSUCML site, where SGD is primarily diffuse and driven mostly by marine forces (Santos et al., 2008a; Smith and Zawadzki, 2003). Taking into account that Alberto was a relatively small storm, the passage of larger, consecutive storms, such as the hurricanes from the 2005 season, could result in more dramatic SGD effects.

3.6. Long-term fluctuations: the influence of precipitation

As discussed earlier, SGD tracer variability over tidal time scales often encompasses most of the long-term spectrum of variation. As we expect no seasonal variability associated with the marine drivers, any seasonal trend may be explained by the terrestrial component of SGD. We initially suspected that high water tables would result in higher SGD tracer concentrations in the coastal ocean. However, the time intervals characterized by anomalously high tracer concentrations are unrelated to high water tables. In general, both the surface aquifer and deep Floridan aquifers have higher levels during the winter than in the summer (Fig. 2). The 30-day smoothed radon and SGD trends did not have a clear seasonal pattern. Relatively lower SGD rates were observed between April and June of 2006 and 2007, while higher values were observed between December 2006 and February 2007. The methane, radon, and radon-derived SGD peaks in December 2006 preceded the shallow and deep aquifer rise by about one month, demonstrating the lack of connection between such variables.

It is difficult to explain the apparent disconnection between SGD and aquifer levels. We speculate that this may be related to a seasonal lag between recharge and discharge, a mechanism suggested for Waquoit Bay (Michael et al., 2005). If this is the case, however, one might expect a freshening of seawater in the summer, which was not observed from our salinity measurements (Fig. 2C). Another, and perhaps more probable, explanation may be related to temporal changes in the tracer cycle and the groundwater endmember concentrations. For example, higher mixing with offshore waters in the winter may lead to lower activities near shore. The higher daily variability in the ^{222}Rn activities observed in the cold months (data not shown) may be associated with higher mixing rates or lower offshore activities. Hence, a temporally constant SGD input associated with a higher groundwater endmember could explain the observed patterns. Unfortunately, we have not made systematic measurements of groundwater nor offshore ^{222}Rn activities to be able to assess these hypotheses.

Scatter plots between shallow groundwater levels and tracer concentrations further indicate no relationships (Fig. 5), suggesting that precipitation and water table height are not primary drivers of SGD at this study site. Throughout the 696 days of measurements, the total precipitation was 1850 mm and concentrated in a few events, including Tropical Storm Alberto (Fig. 13). The average annual precipitation at this area is 1500 mm, so the precipitation during our experiment was only about 65% of the expected value. The period between February and August 2007 was particularly dry, as only one significant precipitation event occurred within six months (45 mm in Apr 2007). Indeed, the drought in Florida during this period was severe. The nearby Ochlocknee River experienced its lowest discharge in 40 years. Hence, the lack of correlation between our SGD tracers and the groundwater table may be partially explained by the overall low precipitation. If this is the case, one might expect to find stronger correlations between the groundwater table and SGD during "normal" years. Despite that, we did record transitions from low to high water tables and even after those few events, we were unable to discern any clear short- (hours to days) or long-term (weeks to months) increase in tracer concentrations or SGD rates in the coastal waters.

Our observations thus offer evidence that seasonal cycles are small compared to short-term fluctuations during this period and that terrestrial processes are not the primary SGD drivers at this coastal plain setting, consistent with a previous numerical model (Smith and Zawadzki, 2003) and salinity observations in seepage meters (Santos et al., 2008a). By interpreting lower frequency observations, other authors found little or no seasonal variations in SGD in certain environments, such as the Baltic Sea (Kaleris et al., 2002), a coastal lagoon from southern Brazil (Santos et al., 2008c), and the Yellow River delta (Peterson et al., 2008). In the Indian River Lagoon, Florida, the lack of correlation between seepage meter-derived advection rates and precipitation indicated that the terrestrial aquifer is not a primary SGD driver (Cable et al., 2006). Other locations, such as volcanic, karstic, and glacial terrains (Garrison et al., 2003; Lee and Kim, 2007), may not be similar, especially if SGD is dominated by freshwater inputs and the hydraulic gradient has a well-defined seasonal cycle. For example, the seasonal hydrologic cycle (higher seawater recharge in the winter) may account for more than 50% of the total SGD fluxes at Waquoit Bay in Massachusetts (Michael et al., 2005). A salt marsh in the same area with steep hydraulic gradients had higher fresh SGD when the water table was elevated (Charette, 2007). Lower excess activities of ^{228}Ra and ^{226}Ra off South Carolina implied lower SGD during the spring and winter (Moore, 2007). In the Pettaquamscutt River estuary (Rhode Island), radium isotope activities followed a sinusoidal pattern of the water table typical of temperate climates, indicating maximum SGD in late spring (Kelly and Moran, 2002).

4. Summary and conclusions

We have reported long-term observations of groundwater tracers at a coastal site in northwestern Florida. Significant correlations between ^{222}Rn and CH_4 indicate that SGD is their major source at this area. We were unable to explain the overall tracer variability as a single function of groundwater table height, rainfall, temperature, tidal fluctuations, and wind speeds, indicating multiple, overlapping controls on SGD dynamics at this site. Precipitation increased the level of the shallow aquifer on time scales of several hours, but had no apparent effect on SGD tracer concentrations measured in the coastal waters. The large spatial and temporal variability in radon and methane in the subterranean estuary demonstrates the complexity of determining SGD endmember concentrations and suggests that unaccounted for temporal changes in the groundwater endmember concentration may explain some of the patterns observed in seawater.

We successfully monitored the passage of various storms during this extended time series. The largest one was strong enough to provide an interesting data set yet not so strong to destroy our equipment, providing a unique opportunity to look into the effects of storms on SGD tracer dynamics. We described a sequence of events in which ^{222}Rn was depleted during the storm and later regenerated to its original concentrations. No influence of the higher post-storm water table could be observed in the ^{222}Rn concentrations.

The range of diurnal variation was generally comparable to, and in many days exceeded the range of seasonal variation of the SGD tracers monitored. Therefore, tidal controls appear to be the dominant driving force at this site. This implies that seasonal investigations of SGD tracers in the coastal ocean may be masked by shorter-term variability, which should be accounted for in future investigations.

Acknowledgements

This project was sponsored by a NSF grant to William Burnett and Jeffrey Chanton (OCE05-20723). Isaac Santos holds a Fulbright/CAPES Ph.D. fellowship (2150/04-2). We thank the Florida State University Coastal and Marine Laboratory (FSUCML) personnel for their helpful support.

References

Avila, L.A., Brown, D.P., 2006. Tropical cyclone report. Tropical Storm Alberto 10–14 June 2006. National Hurricane Center.

Beck, A.J., Rapaglia, J.P., Cochran, J.K., Bokuniewicz, H.J., 2007. Radium mass-balance in Jamaica Bay, NY: evidence for a substantial flux of submarine groundwater. Marine Chemistry 106 (3–4), 419–441.

Bugna, G.C., Chanton, J.P., Cable, J.E., Burnett, W.C., Cable, P.H., 1996. The importance of groundwater discharge to the methane budgets of nearshore and continental shelf waters of the northeastern Gulf of Mexico. Geochimica et Cosmochimica Acta 60 (23), 4735–4746.

Burnett, W., Bokuniewicz, H., Huettel, M., Moore, W.S., Taniguchi, M., 2003. Groundwater and pore water inputs to the coastal zone. Biogeochemistry 66 (3), 3–33.

Burnett, W., Kim, G., Lane-Smith, D., 2001. A continuous monitor for assessment of 222Rn in the coastal ocean. Journal of Radioanalytical and Nuclear Chemistry 249 (1), 167–172.

Burnett, W.C., Aggarwal, P.K., Aureli, A., Bokuniewicz, H., Cable, J.E., Charette, M.A., Kontar, E., Krupa, S., Kulkarni, K.M., Loveless, A., et al., 2006. Quantifying submarine groundwater discharge in the coastal zone via multiple methods. Science of the Total Environment 367 (2–3), 498–543.

Burnett, W.C., Dulaiova, H., 2003. Estimating the dynamics of groundwater input into the coastal zone via continuous radon-222 measurements. Journal of Environmental Radioactivity 69 (1–2), 21–35.

Burnett, W.C., Peterson, R., Moore, W.S., Oliveira, J., 2008. Radon and radium isotopes as tracers of submarine groundwater discharge — results from the Ubatuba, Brazil SGD assessment intercomparison. Estuarine, Coastal and Shelf Science 76, 501–511.

Burnett, W.C., Santos, I.R., Weinstein, Y., Swarzenski, P.W., Herut, B., 2007. Remaining uncertainties in the use of Rn-222 as a quantitative tracer of submarine groundwater discharge. In: Sanford, W., Langevin, C., Polemio, M., Povinec, P. (Eds.), A New Focus on Groundwater–Seawater Interactions, vol. 312. IAHS Publ., Perugia, Italy, pp. 109–118.

Cable, J.E., Bugna, G.C., Burnett, W., Chanton, J.P., 1996a. Application of 222Rn and CH4 for assessment of groundwater discharge to the coastal ocean. Limnology and Oceanography 41 (6), 1347–1353.

Cable, J.E., Burnett, W., Chanton, J.P., 1997. Magnitude and variations of groundwater seepage along a Florida marine shoreline. Biogeochemistry 38, 189–205.

Cable, J.E., Burnett, W.C., Chanton, J.P., Weatherly, G.L., 1996b. Estimating groundwater discharge into the northeastern Gulf of Mexico using radon-222. Earth and Planetary Science Letters 144 (3–4), 591–604.

Cable, J.E., Martin, J.B., Corbett, D., 2006. Exonerating Bernoulli? On evaluating the physical and biological processes affecting marine seepage meter measurements. Limnology and Oceanography Methods 4, 172–183.

Chanton, J.P., Burnett, W., Dulaiova, H., Corbett, D., Taniguchi, M., 2003. Seepage rate variability in Florida Bay driven by Atlantic tidal height. Biogeochemistry 66, 187–202.

Charette, M., Moore, W.S., Burnett, W.C., 2008. Uranium- and thorium-series nuclides as tracers of submarine groundwater discharge. Radioactivity in the Environment, vol. 13. Elsevier, pp. 155–191.

Charette, M.A., 2007. Hydrologic forcing of submarine groundwater discharge: insight from a seasonal study of radium isotopes in a groundwater-dominated salt marsh estuary. Limnology and Oceanography 52 (1), 230–239.

Corbett, D., Burnett, W., Cable, J.E., Clark, S.B., 1998. A multiple approach to the determination of radon fluxes from sediments. Journal of Radioanalytical and Nuclear Chemistry 236, 247–252.

Dulaiova, H., Burnett, W.C., Chanton, J.P., Moore, W.S., Bokuniewicz, H.J., Charette, M.A., Sholkovitz, E., 2006. Assessment of groundwater discharges into West Neck Bay, New York, via natural tracers. Continental Shelf Research 26 (16), 1971–1983.

Dulaiova, H., Gonneea, M.E., Henderson, P.B., Charette, M.A., 2008. Geochemical and physical sources of radon variation in a subterranean estuary — implications for groundwater radon activities in submarine groundwater discharge studies. Marine Chemistry 110 (1–2), 120–127.

Garcia, M.L., Masson, M., 2004. Environmental and geologic application of solid-state methane sensors. Environmental Geology 46, 1059–1063.

Garrison, G.H., Glenn, C.R., McMurtry, G.M., 2003. Measurement of submarine groundwater discharge in Kahana Bay, O ahu, Hawaii. Limnology and Oceanography 48 (2), 920–928.

Gonneea, M.E., Morris, P.J., Dulaiova, H., Charette, M.A., 2008. New perspectives on radium behavior within a subterranean estuary. Marine Chemistry 109 (3–4), 250–267.

Grunwald, M., Dellwig, O., Liebezeit, G., Schnetger, B., Reuter, R., Brumsack, H.J., 2007. A novel time-series station in the Wadden Sea (NW Germany): first results on continuous nutrient and methane measurements. Marine Chemistry 107 (3), 411–421.

Hougham, A.L., Moran, S.B., Masterson, J.P., Kelly, R.P., 2008. Seasonal changes in submarine groundwater discharge to coastal salt ponds estimated using 226Ra and 228Ra as tracers. Marine Chemistry 109 (3–4), 268–278.

Hu, C., Muller-Karger, F.E., Swarzenski, P.W., 2006. Hurricanes, submarine groundwater discharge, and Florida's red tides. Geophysical Research Letters 33, L11601. doi:10.1029/2005GL025449.

Kaleris, V., Lagas, G., Marczinek, S., Piotrowski, J.A., 2002. Modelling submarine groundwater discharge: an example from the western Baltic Sea. Journal of Hydrology 265 (1–4), 76–99.

Kelly, R.P., Moran, S.B., 2002. Seasonal changes in groundwater input to a well-mixed estuary estimated using radium isotopes and implications for coastal nutrient budgets. Limnology and Oceanography 47, 1807–1976.

Kim, G., Hwang, D.W., 2002. Tidal pumping of groundwater into the coastal ocean revealed from submarine Rn-222 and CH4 monitoring. Geophysical Research Letters 29 (14). doi:10.1029/2002GL015093.

Kroeger, K.D., Swarzenski, P.W., Greenwood, W.J., Reich, C., 2007. Submarine groundwater discharge to Tampa Bay: nutrient fluxes and biogeochemistry of the coastal aquifer. Marine Chemistry 104 (1–2), 85–97.

Lambert, M., Burnett, W., 2003. Submarine groundwater discharge estimates at a Florida coastal site based on continuous radon measurements. Biogeochemistry 66, 55–73.

Lapointe, B.E., Barile, P.J., Littler, M.M., Littler, D.S., 2005. Macroalgal blooms on southeast Florida coral reefs: II. Cross-shelf discrimination of nitrogen sources indicates widespread assimilation of sewage nitrogen. Harmful Algae 4 (6), 1106–1122.

Lee, J.M., Kim, G., 2007. Estimating submarine discharge of fresh groundwater from a volcanic island using a freshwater budget of the coastal water column. Geophysical Research Letters 34 (11), L11611. doi:10.1029/2007GL029818.

Li, H., Jiao, J.J., 2003. Tide-induced seawater–groundwater circulation in a multi-layered coastal leaky aquifer system. Journal of Hydrology 274 (1–4), 211–224.

Loveless, A.M., Oldham, C.E., Hancock, G.J., 2008. Radium isotopes reveal seasonal groundwater inputs to Cockburn Sound, a marine embayment in Western Australia. Journal of Hydrology 351 (1–2), 203–217.

Michael, H.A., Mulligan, A.E., Harvey, C.F., 2005. Seasonal oscillations in water exchange between aquifers and the coastal ocean. Nature 436, 1145–1148.

Moore, W.S., 1997. High fluxes of radium and barium from the mouth of the Ganges–Brahmaputra River during low river discharge suggest a large groundwater source. Earth and Planetary Science Letters 150 (1–2), 141–150.

Moore, W.S., 2003. Sources and fluxes of submarine groundwater discharge delineated by radium isotopes. Biogeochemistry 66, 75–93.

Moore, W.S., 2007. Seasonal distribution and flux of radium isotopes on the southeastern U.S. continental shelf. Journal of Geophysical Research 112, C10013. doi:10.1029/2007JC004199.

Moore, W.S., Blanton, J.O., Joye, S.B., 2006. Estimates of flushing times, submarine groundwater discharge, and nutrient fluxes to Okatee Estuary, South Carolina. Journal of Geophysical Research 111, C09006. doi:10.1029/2005JC003041.

Moore, W.S., Sarmiento, J.L., Key, R.M., 2008. Submarine groundwater discharge revealed by 228Ra distribution in the upper Atlantic Ocean. Nature Geosciences 1, 309–311.

Moore, W.S., Wilson, A.M., 2005. Advective flow through the upper continental shelf driven by storms, buoyancy, and submarine groundwater discharge. Earth and Planetary Science Letters 235 (3–4), 564–576.

Mulligan, A.E., Charette, M.A., 2006. Intercomparison of submarine groundwater discharge estimates from a sandy unconfined aquifer. Journal of Hydrology 327 (3–4), 411–425.

Peterson, R.N., Burnett, W.C., Taniguchi, M., Chen, J., Santos, I.R., Ishitobi, T., 2008. Radon and radium isotope assessment of submarine groundwater discharge in the Yellow River Delta, China. Journal of Geophysical Research 113, C09021. doi:10.1029/2008JC004776.

Santos, I.R., Burnett, W., Chanton, J.P., Mwashote, B., Suryaputra, I.G.N.A., Dittmar, T., 2008a. Nutrient biogeochemistry in a Gulf of Mexico subterranean estuary and groundwater-derived fluxes to the coastal ocean. Limnology and Oceanography 53 (2), 705–718.

Santos, I.R., Machado, M.I., Niencheski, L.F., Burnett, W., Milani, I.B., Andrade, C.F.F., Peterson, R.N., Chanton, J., Baisch, P., 2008b. Major ion chemistry in a freshwater coastal lagoon from southern Brazil (Mangueira Lagoon): influence of groundwater inputs. Aquatic Geochemistry 14, 133–146. doi:10.1007/s10498-008-9029-0.

Santos, I.R., Niencheski, F., Burnett, W., Peterson, R., Chanton, J.P., Andrade, C.F.F., Milani, I.B., Schmidt, A., Knoeller, K., 2008c. Tracing anthropogenically driven groundwater discharge into a coastal lagoon from southern Brazil. Journal of Hydrology 353 (3–4), 275–293. doi:10.1016/j.jhydrol.2008.02.010.

Sholkovitz, E.R., Herbold, C., Charette, M.A., 2003. An automated dye-dilution based seepage meter for the time-series measurement of submarine groundwater discharge. Limnology and Oceanography: Methods 1, 17–29.

Slomp, C.P., Van Cappellen, P., 2004. Nutrient inputs to the coastal ocean through submarine groundwater discharge: controls and potential impact. Journal of Hydrology 295 (1–4), 64–86.

Smetacek, V., Cloern, J.E., 2008. On phytoplankton trends. Science 319 (5868), 1346–1348.

Smith, C.G., Cable, J.E., Martin, J.B., 2008. Episodic high intensity mixing events in a subterranean estuary: effects of tropical cyclones. Limnology and Oceanography 53 (2), 666–674.

Smith, L., Zawadzki, W., 2003. A hydrogeologic model of submarine groundwater discharge: Florida intercomparison experiment. Biogeochemistry 66 (1–2), 95–110.

Swarzenski, P.W., 2007. U/Th series radionuclides as coastal groundwater tracers. Chemical Reviews 107 (2), 663–674.

Swarzenski, P.W., Reich, C.D., Spechler, R.M., Kindinger, J.L., Moore, W.S., 2001. Using multiple geochemical tracers to characterize the hydrogeology of the submarine spring off Crescent Beach, Florida. Chemical Geology 179 (1–4), 187–202.

Swarzenski, P.W., Simonds, F.W., Paulson, A.J., Kruse, S., Reich, C., 2007. Geochemical and geophysical examination of submarine groundwater discharge and associated nutrient loading estimates into Lynch Cove, Hood Canal, WA. Environmental Science and Technology 41, 7022–7029.

Taniguchi, M., 2002. Tidal effects on submarine groundwater discharge into the ocean. Geophysical Research Letters 29 (12) Art. No. 1561.

Taniguchi, M., Iwakawa, H., 2004. Submarine groundwater discharge in Osaka Bay, Japan. Limnology 5 (1), 25–32.

Taniguchi, M., Stieglitz, T., Ishitobi, T., 2008. Temporal variability of water quality of submarine groundwater discharge in Ubatuba, Brazil. Estuarine, Coastal and Shelf Science 76 (3), 484–492.

Weinstein, Y., Burnett, W.C., Swarzenski, P.W., Shalem, Y., Yechieli, Y., Herut, B., 2007. Role of aquifer heterogeneity in fresh groundwater discharge and seawater recycling: an example from the Carmel coast, Israel. Journal of Geophysical Research 112, C12016. doi:10.1029/2007JC004112.

Yamamoto, S., Alcauskas, J.B., Crozier, T.E., 1976. Solubility of methane in distilled water and seawater. Journal of Chemical and Engineering Data 21 (1), 78–80.

Zektser, I.S., Loaiciga, H.A., 1993. Groundwater fluxes in the global hydrologic cycle: past, present and future. Journal of Hydrology 144, 405–427.